Geology and petrogenesis of magmatic veins at El Porticito volcanic vent, Catron County

Robert R. Horning, Nelia W. Dunbar, W. Scott Baldridge, and Philip R. Kyle

2003, pp. 139-154. https://doi.org/10.56577/FFC-54.139

in:

Geology of the Zuni Plateau, Lucas, Spencer G.; Semken, Steven C.; Berglof, William; Ulmer-Scholle, Dana; [eds.], New Mexico Geological Society 54 th Annual Fall Field Conference Guidebook, 425 p.
https://doi.org/10.56577/FFC-54

This page is intentionally left blank to maintain order of facing pages.

New Mexico Geological Society Guidebook, 54th Field Conference, Geology of the Zuni Plateau, 2003, p. 139-154.

GEOLOGY AND PETROGENESIS OF MAGMATIC VEINS AT EL PORTICITO VOLCANIC VENT, CATRON COUNTY, NEW MEXICO

ROBERT R. HORNING[1], NELIA W. DUNBAR[2], W. SCOTT BALDRIDGE[3] AND PHILIP R. KYLE[2]
[1]P.O. Box 460, Tesuque, NM 87574, rrhorning@cybermesa.com; [2]New Mexico Bureau of Geology and Mineral Resources, 801 Leroy Place, Socorro, NM 875801; [3]Los Alamos National Laboratory, P.O. Box 1663, Los Alamos, NM 87545

Abstract.—El Porticito is the approximately 70-m high eroded remnant of a 7.08 ± 0.25 Ma volcanic vent located in the transition zone between the Colorado Plateau and the Basin and Range province in west-central New Mexico. It is distinguished by the strikingly white, vertical and horizontal, centimeter- to meter-scale, magmatic veins that cut across the black faces of the edifice. At nearby Tejana Mesa, a latticework of centimeter-scale subvertical veins merges upward into a single 10-m thick white sill that extends some 200 m along the cliff face. El Porticito consists primarily of two basanites. The late basanite has more Al_2O_3 and less MgO and compatible trace elements, indicating that it is more evolved than the early basanite. Residuals calculated during mass balance modeling of crystal fractionation suggest that the second basanite probably did not evolve from the early basanite. Instead, similar rare earth element concentrations and identical ε_{Nd} (+3.2) suggest that the two basanites evolved from a common mantle parent. Although concentrations are near detection limits, the lower calcium contents of the cores of olivine phenocrysts found in the late basanite suggest that equilibration between olivine cores and surrounding melt occurred at greater depth than in the early basanite.

Geochemical modeling, using major and trace element data, suggests that vein magma probably evolved at shallow depth through crystal fractionation from the older, less-evolved basanite. However, the solutions of the models are close enough that the possibility remains that the veins evolved from the later-erupted, less evolved basanite. Veins occur only within the late basanite, except in one small volume at Tejana Mesa where they extend less than a meter into the early basanite. Partially and entirely detached xenoliths of wall rock found in veins are compatible with forceful intrusion of vein magma into its host. The existence of both smooth trajectories and abrupt, right angle changes in vein orientation suggest that vein magma intruded the younger basanite at presently exposed levels while the basanite cooled through the rheological critical melt percentage and behaved as both a ductile and brittle host, depending upon its degree of crystallinity at a particular location.

INTRODUCTION

Veins and pods of evolved silicate rocks are found within a variety of crystalline host bodies. (Here we use the term "vein" to denote a thin igneous intrusion found in an igneous host. No particular orientation is implied.) Such veins occur in the Shonkin Sag laccolith, Montana (Barksdale, 1937; Barksdale, 1952; Hurlbut and Griggs, 1939); Antarctic diabases (Hamilton et al., 1965); the Slaufrudalur granophyre intrusion, Iceland (Saemundsson, 1979); the Makaopuhi and Kilauea Iki lava lakes, Hawaii (Peterson and Moore, 1987); the flood basalts of the Hartford Basin, Connecticut (Philpotts, et al., 1996); and the Columbia River Basalt province, Washington (Puffer and Horter, 1993).

The formation of magmatic veins and pods depends upon three processes: evolution and separation of vein magma from its source, transport to its destination, and emplacement into space created in the host. Common sources of vein magmas include the mush of the lower (Marsh et al., 1991) and upper (Helz et al., 1989) solidification zones of crystallizing bodies. Mechanisms involved in separation of vein melt from a solidification zone include crystal mush compaction, i.e., filter pressing (Helz et al., 1989), and upward or lateral porous flow of low density liquid through the crystal mush (Philpotts et al., 1996).

Ascent of relatively low-density vein magma to the zone of emplacement may be facilitated by (1) the formation of diapirs that rise through intervening melt or along magma chamber walls, as in La Gloria pluton, Chile, (Mahood and Cornejo, 1992) and Kilauea Iki lava lake (Helz et al., 1989); (2) entrainment of melt in streams of vesicles propagating through intervening melt (Helz et al., 1989, Puffer and Horter, 1993); and (3) formation of vertical pipes through nearly solid magma, as at Shonkin Sag (Marsh et al., 1991).

Space needed for vein emplacement is provided by dilation and formation of cracks within, or beyond, the solidification front of a host magma body. These cracks may result when pore pressure exceeds the tensile strength of the crystal mush (Philpotts and Carroll, 1996), by thermal contraction of crystallizing magma, by gravity-induced tearing of the crystal mush, or by detachment and foundering of solid roof rock (Marsh et al., 1991).

The present study area has heretofore received little attention. El Porticito is included in the 30 X 60 minute map of the Quemado quadrangle (Chamberlin et al., 1994). Guilinger (1982) performed a geologic study of the Tejana Mesa area, NE of El Porticito; his study emphasized the origin of uranium occurrences near Mesa Tinaja. He also observed the "graben-like" feature in which El Porticito is located, and the latter's "dike-like geometry".

Baldridge et al. (1989) and Baldridge (1994) briefly described the volcanic stratigraphy of El Porticito and adjacent Tejana Mesa and the vein petrography and the compositions of vein minerals. They noted particularly the textures that distinguish veins from host lavas. Many veins have textures that are considerably more coarse than their host magma bodies. Baldridge et al. (1989) concurred with Guilinger (1982) that the physical relationships of the stratigraphic units in the vicinity of El Porticito suggest that the lavas filled a depression in underlying sediments or ponded in a lava lake inside a tuff ring. Baldridge (1994) suggested that the veins of El Porticito and nearby Tejana Mesa may be either the product of melt segregation from the surrounding crystallizing host magma or of intrusion of melts into the host from a separate, deeper magma source.

Two previous studies have reported ages for the volcanic rocks of El Porticito and nearby Tejana Mesa. Dethier et al. (1986) obtained a K-Ar age of 6.73 ± 0.18 Ma for volcanic rocks capping Tejana Mesa about 1.1 km NE of El Porticito. More recently, McIntosh

and Cather (1994) reported an $^{40}Ar/^{39}Ar$ plateau age of 7.92 ± 0.40 Ma (2σ) for a whole rock sample (nm1104), with the composition of the late basanite of this study, taken from El Porticito.

Here, in addition to presenting new age data, we describe the rocks and their physical relationships, and attempt to develop a model that explains the most likely mechanisms for the generation of host and vein magmas, and for their emplacement at El Porticito and adjacent Tejana Mesa.

GEOLOGIC SETTING

El Porticito is located in the transition zone (Aldrich and Laughlin, 1984; Baldridge et al., 1991; Menzies et al., 1991) between the Colorado Plateau and the Basin and Range province in west-central New Mexico. It lies near the southern margin of the Jemez Lineament (Chapin et al., 1978), an alignment of volcanic centers extending northeast from the White Mountains of eastern Arizona, across the Rio Grande Rift, to the Raton-Clayton Volcanic Field of northeastern New Mexico. The lineament has been interpreted as coinciding with the buried boundary between the Proterozoic Yavapai and Mazatzal crustal provinces (Karlstrom and Bowring, 1993; Karlstrom and Daniel, 1993).

Minier and Reiter (1991) observed anomalously high heat flow in numerous shallow wells in the central Jemez Lineament. The high heat flow may be related to the Tejana vent zone, which consists of 10 vents, including El Porticito, extending about 15 km SW from Mesa Tinaja. R. M. Chamberlin (personal commun., 2003) has interpreted this zone as the surface expression of a northeast-striking feeder dike system.

METHODS AND ANALYTICAL PROCEDURES

Tephra samples were collected from outcrops near the base of the northwest and southeast corners of Tejana Mesa (Fig. 1). Basanite samples were collected along the base and top of Tejana Mesa and from all sides of El Porticito. Vein samples were collected along the base of Tejana Mesa and from exposures throughout El Porticito. Overall, sampling was random, except where stratigraphic or structural features appeared to be anomalous, suggesting that additional sampling would be useful.

Mineral compositions in thin sections of representative rock specimens taken from El Porticito and nearby Tejana Mesa were determined employing standard procedures with a Caméca model SX50 electron microprobe at the Los Alamos National Laboratory using a 10 μm diameter, 10 nA, 15 kV beam. Calibrations were performed using several natural and synthetic standards. Matrix effects were corrected using the PAP procedure (Pouchou and Pichoir, 1985); and the manufacturer's software was used to calculate elemental and oxide concentrations.

In preparation for whole rock chemical analyses, three hundred g to 1 kg splits, depending upon maximum grain size in the sample, were crushed with a steel jaw crusher. Selected samples were then subjected to repeated leaching in 3% acetic acid solutions until effervescence ceased, to remove any calcite that might be present. After drying at 100˚C for at least 1 hour, samples were ground to 10 μm, or finer, powder using a tungsten carbide swing mill.

Whole rock compositional analyses were performed at the New Mexico Institute of Mining and Technology (NMT) X-ray Fluorescence Lab employing a Philips model PW2400 XRF spectrometer on fused disks for major element oxides, and pressed powder pellets for V, Ni, Cu, Zn, Ga, Rb, Sr, Y, Zr, Nb, Mo, Ba, and Pb (Norrish and Chappell, 1977; Hallett and Kyle, 1993). The trace elements Sc, Cr, As, Sb, Cs, La, Ce, Nd, Sm, Eu, Tb, Yb, Lu, Hf, Ta, Th, and U were measured by INAA at NMT after irradiation of samples at the University of Missouri Research Reactor for 24 hours using a neutron flux density of 2.5×10^{13} $n\cdot cm^{-2}\cdot s^{-1}$. Samples were counted using two high purity Ge detectors (with resolutions of 1.8 kev at 1332 kev and 25% efficiency) 7 to 10 and 30 to 40 days following irradiation. NIST standard SRM 1633a was used for calibration (Hallett and Kyle, 1993).

O. T. Rämö performed neodymium isotopic analyses at the Unit for Isotope Geology, Geological Survey of Finland. For a description of the analytical procedures, see Luttinen et al. (1998).

Sample whole rock $^{40}Ar/^{39}Ar$ ages were obtained at New Mexico Tech's Geochronology Laboratory. Samples were crushed, packaged in fused silica vials, and irradiated for 1 hr at the University of Michigan's Ford Research Reactor, using Fish Canyon Tuff sanidine, with an assigned age of 27.84 Ma, as a neutron flux monitor. Irradiated samples were then step-heated and analyzed using a Mass Analyzer Products 215-50 mass spectrometer, operated in static mode.

FIELD RELATIONSHIPS

El Porticito is a ~70-m high, elongate butte located approximately 8 km NW of Quemado, New Mexico (Fig. 1). It is composed of erupted mafic lavas. Northeast, across Largo Creek, mafic lavas also cap Tejana Mesa. Tejana Mesa is somewhat higher than El Porticito, and extends northwest ≈ 10 km. The portion of Tejana Mesa included in Figure 1 is but a small NE-oriented protrusion of its SW corner.

El Porticito

This butte consists primarily of two fine-grained, melanocratic basanite units, the older mapped as "Tepb1", and the younger as "Tepb2". Both basanite units are fine grained and generally structureless. In outcrop and hand specimen, these units have very similar color and mineralogy; but can be distinguished by weathered surface textures. The older basanite has a relatively fresh appearance and smoothly weathered surfaces. Near the S end of the E side of El Porticito, it exhibits a strong joint pattern, with joints striking ~N7˚E and dipping ~80˚E. The younger basanite usually has a rough, knobby, weathered surface. The contact between the two basanite units is approximately vertical on the E side of El Porticito (Fig. 2); and there is no evidence that suggests significant tilting of this contact since emplacement of the basanites.

The feature of El Porticito that distinguishes it from many other eroded volcanic vents is the presence of numerous anastomosing, white tephrite/phonotephrite veins, mapped as "Tepv", that cut the dark basanite. The veins range in orientation from vertical to horizontal and in thickness from ≤1 cm to ≥2 m. Large arrays of

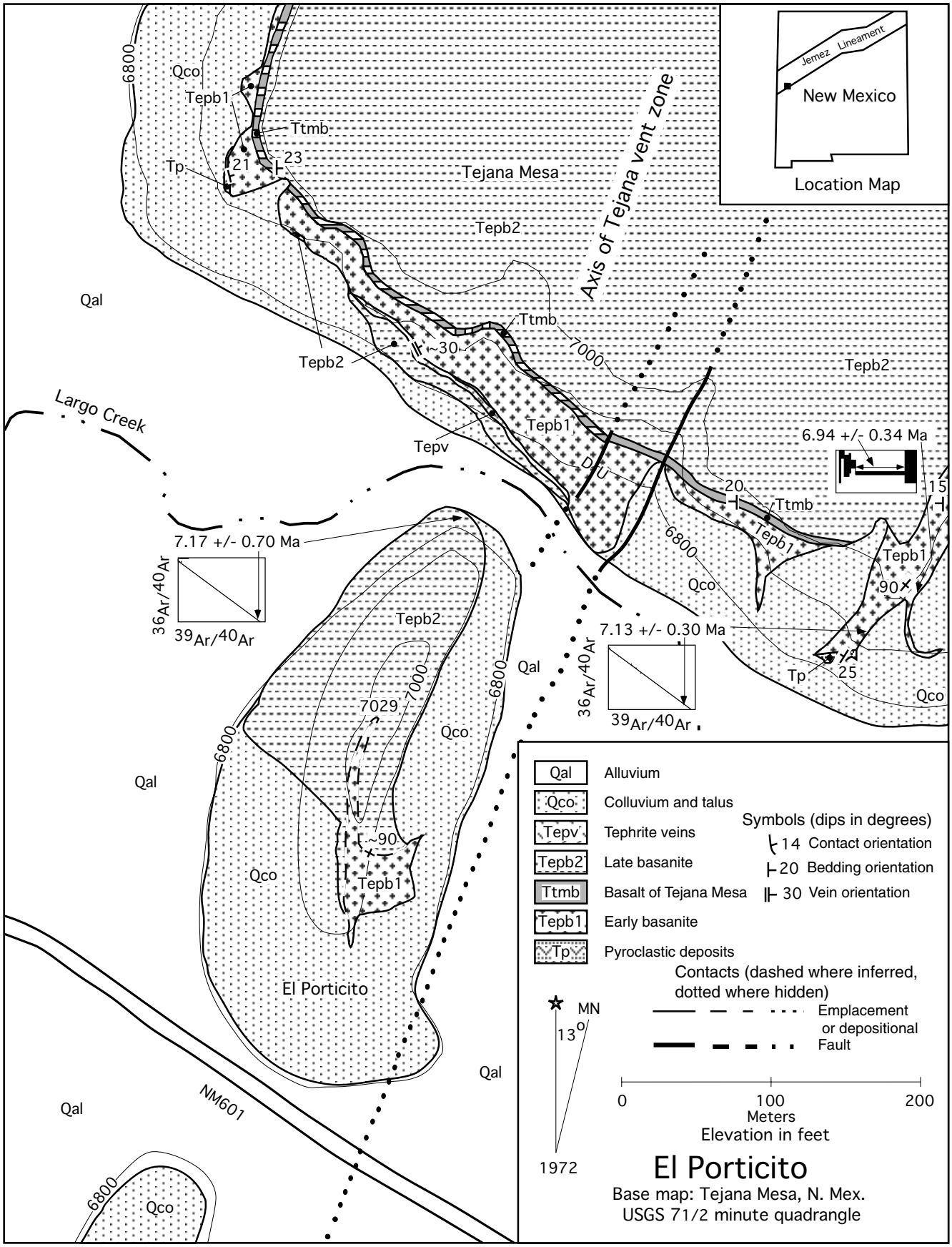

FIGURE 1. Geologic map of El Porticito and nearby Tejana Mesa. The portion of Tejana Mesa included in the study area is a small projection of the landform, which extends to the north approximately 10 km.

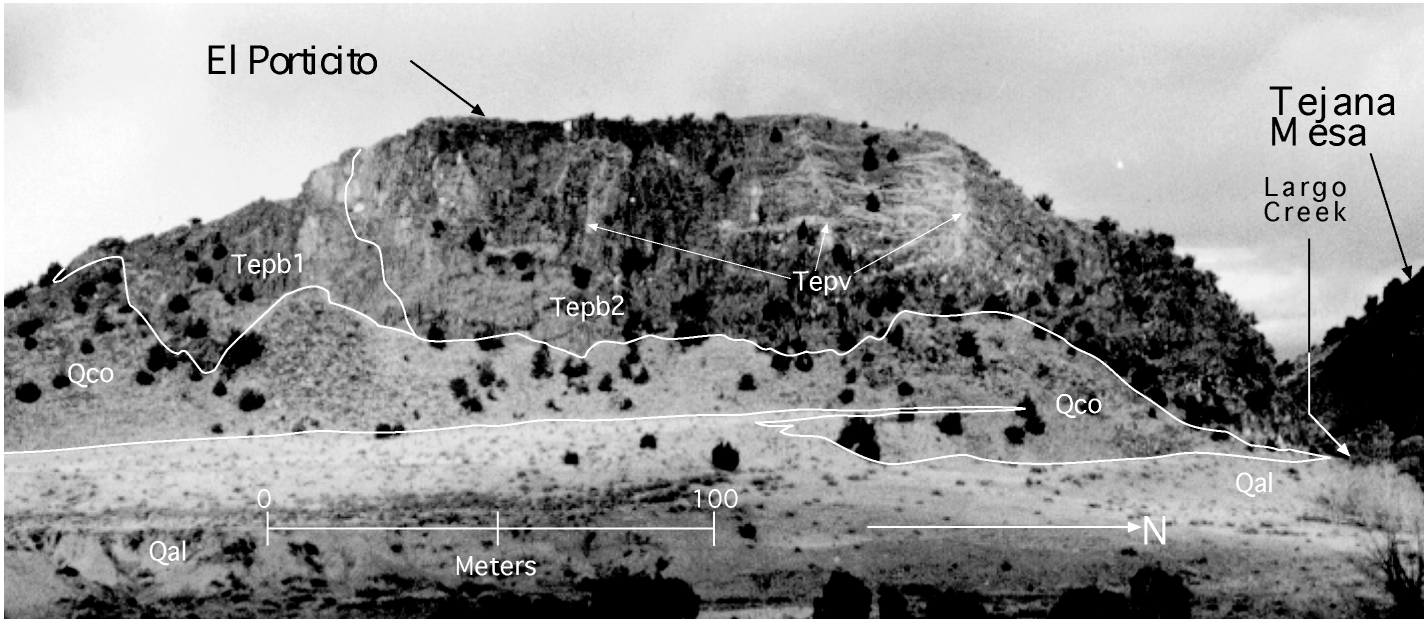

FIGURE 2. The east face of El Porticito. Unit symbols are from Figure 1. Only the largest tephrite dike- and sill-like veins (white streaks labeled "Tepv") are visible in the black basanite host rock. Veins only occur in the late, more evolved basanite, labeled "Tepb2". This late basanite also contains horizontal, submillimeter, silicate veinlets, which appear to be responsible for the rock's knobby surface texture. The early basanite, "Tepb1", is smooth. Note the near-vertical contact between the early and late basanites.

veins are present in the northern portion of the outcrop, and smaller arrays are found to the south. Horizontal vein thickness increases upward, reaching a maximum about 85% of the way up the E side of El Porticito. Above this level, thickness decreases dramatically; and at the top veins are generally ≤1 cm thick. Beneath and between these horizontal arrays are subvertical veins of generally lesser thickness. Subvertical veins occasionally form upward-merging dendritic patterns beneath horizontal arrays. Most veins follow smoothly-curved paths through the host, but in at least one location a vein twice changes orientation abruptly (Horning, 1997).

Many veins exhibit magmatic flow foliations defined by linear concentrations of phenocrysts. Partially to completely detached xenoliths of late basanite, some decimeters in length, can be seen in outcrop and thin section included in veins. Very small, mafic crystals that apparently nucleated and grew in place along the vein-wall rock interface can also be seen. Thin cracks, usually filled by silicate phases, are frequently observed following vein-wall rock interfaces.

Leucocratic silicate veinlets, typically <0.2 mm in thickness and a few cm in length, are common throughout the younger basanite, and probably account for its knobby appearance. These veinlets occasionally cross vein-wall rock interfaces, but more often grade into veins. All observed veinlets have a horizontal orientation, and are composed of silicate phases.

Tejana Mesa

The stratigraphically lowest volcanic rocks in the study area consist of poorly-consolidated pyroclastic deposits, most of which include abundant accessory and accidental clasts. The latter include sparse felsic pumice and abundant quartzite. The tephras are mapped as "Tp" (Fig. 1). Outside the study area, the top of country rock (Fence Lake Formation) exists ~25 m above the highest exposure of pyroclastic deposits at Tejana Mesa, suggesting that the tephra were erupted into a previously excavated volcanic crater or into a paleovalley. Internal structures, including scoured, U-shaped troughs and local trough cross bedding, (Horning, 1997) are interpreted to indicate that tephra are wet and dry surge deposits (Cas and Wright, 1993) that probably formed part of a tuff ring.

Overlying the pyroclastic deposits is aphanitic early basanite with upper and lower vesicular zones (Aubele et al., 1988) and a brecciated base. A separate dike and thin flow with the composition of early basanite crops out atop the SE corner of Tejana Mesa.

The basalt of Tejana Mesa (informal name), here mapped as "Ttmb", is the "entablature" of Baldridge, et al., 1989. It is interpreted here to be a separate flow that rests upon the originally level upper surface of the early basanite. It is generally about 9 m thick, exhibits an autobrecciated, vesiculated upper surface, and underlies a narrow bench. The bench, and underlying flow, slope toward a fault seen on the SW face of Tejana Mesa. East of the fault, the basalt dips west and the bench is quite prominent. West of the fault, the flow dips east and outcrops are discontinuous, tending to be covered by talus. The western strand of the fault offsets the flow, down to the west, but apparently not the lava above it. Unfortunately, the basalt of Tejana Mesa has not undergone geochemical analysis.

Late basanite overlies the basalt of Tejana Mesa. No veins have been observed in this late basanite flow, but a few veinlets occur in it near the SW corner of Tejana Mesa. The late basanite flow thickens markedly toward the fault at Tejana Mesa, probably

TABLE 1. Generalized petrographic summary of El Porticito and adjacent Tejana Mesa volcanic units

Rock Type	Unit	Texture	Ol	Aug	TAug	FT	Hem	Ksp	Ano	Ne	Ap	Ana	Ser	Zeo	Cla	Ca	Gl
Bombs	Tp	ves, amg, mp (<5)	a	a		g, p		tr							p	p	g, a
Basanite lava	Tepb1	fg,fp, str,ves, str,fb (<5)	a	a	p	p		g, tr				g, tr			g, tr	g, tr	
Melano-cratic lava	Ttmb	ves, fb															g, a(?)
Basanite lava	Tepb2	mp,fp, str,ves, str,fb, (<5)	a	a	a	p,a		g, p,a		g, tr	tr	g, tr,p	g, tr		g, tr		g, p(?)
Tephrite veins	Tepv	fp,cp, str,fl (20 - 60)		tr	p,a	p,a	tr	g, a	tr	g, p	g, p	g, p,a	g, p,a	g, tr,a	g, tr,p	g, tr	

abbreviations: *minerals* Ol = olivine; Aug = augite; TAug = Titanaugite; FT = Fe-Ti oxides; Hem = hematite; Ksp = potassic feldspar; Ano = anorthoclase; Ne = nepheline; Ap = apatite; Ana = analcime; Ser = sericite; Zeo = zeolites; Cla = clay; Ca = calcite; Gl = glass or very fine-grained matrix
concentrations tr = trace (≤1%); p = present (>1%); a = abundant (>10%); g = groundmass only
textures amg = amygdaloidal; ves = vesicular; str = structureless; fb = flow brecciated; fl = flow lineations; cp = coarsely porphyritic (phenos >5 mm); fg = fine grained, fp = finely porphyritic (phenos >2 mm); mp = microporphyritic (<2 mm). Proportion of phenocrysts >2 mm is given to nearest 5% in parentheses.

indicating that this flow filled a structurally-controlled paleovalley underlain by the basalt of Tejana Mesa.

Late basanite also crops out locally at the upper boundary of colluvium and talus beneath early basanite west of the fault at Tejana Mesa. Because the lower contact of this late basanite outcrop is hidden, it is unclear whether it intruded beneath, or into, early basanite. A complex of leucocratic veins, chemically and texturally indistinguishable from veins at El Porticito, cut this late basanite at a high angle and merge upward to form a ≤10-m thick leucocratic sill at the exposed contact between late and early basanites. Rarely, centimeter-scale veins extend above the leucocratic sill into the overlying early basanite. The sill pinches out toward the northwest and repeatedly breaks up into thinner strands toward the southeast.

Eruptive Sequence

In summary, the first eruptive products were the pyroclastic deposits now found at Tejana Mesa. Early basanite occurs in El Porticito and as a flow lying atop the tephra at Tejana Mesa. The basalt of Tejana Mesa rests upon early basanite. Late basanite exists beside early basanite at El Porticito. Late basanite also flowed over the basalt of Tejana Mesa, and intruded beneath early basanite at Tejana Mesa. Thus the late basanite followed the early basanite and the basalt of Tejana Mesa. At Tejana Mesa, veins intrude both the lower outcrop of late basanite and the overlying early basanite, indicating that vein intrusion postdated both basanite lavas.

RESULTS

Petrography and Mineral Chemistry

The lavas at El Porticito are mostly holocrystalline and microporphyritic, and consist mainly of groundmass augites, Fe-Ti oxides, and minor potassium feldspars, with phenocrysts of olivine and augite (Horning, 1997). In contrast, the veins are holocrystalline and phaneritic, and consist of large Ti-augite and Fe-Ti oxide phenocrysts in a matrix of alkali feldspar, pyroxene, Fe-Ti oxides, analcime, leucite, sericite, and apatite. Table 1 lists a summary of the petrography of El Porticito and Tejana Mesa volcanic rocks.

Within olivine phenocrysts of the early and late basanite lavas, concentrations of both CaO and MnO, which are indicators of crystallization environments (Stormer, 1973), increase from cores to rims. Concentrations in rims are similar to groundmass grain concentrations. MnO concentrations in late basanite olivine phenocryst rims and groundmass grains are somewhat higher than those in early basanite (Fig. 3). A summary of representative mineral compositions is listed in Table 2.

Whole Rock Geochemistry and Dating

The major element compositions of rocks found at El Porticito and Tejana Mesa progressively changed during the eruptive sequence (Table 3). Compositions became more evolved, beginning with the picrobasalts and foidites of tephra and ending with the tephrites and phonotephrites of veins. Trends of Al_2O_3, TiO_2, and Ni in tephra are notably different from those in the basanites (Fig. 4).

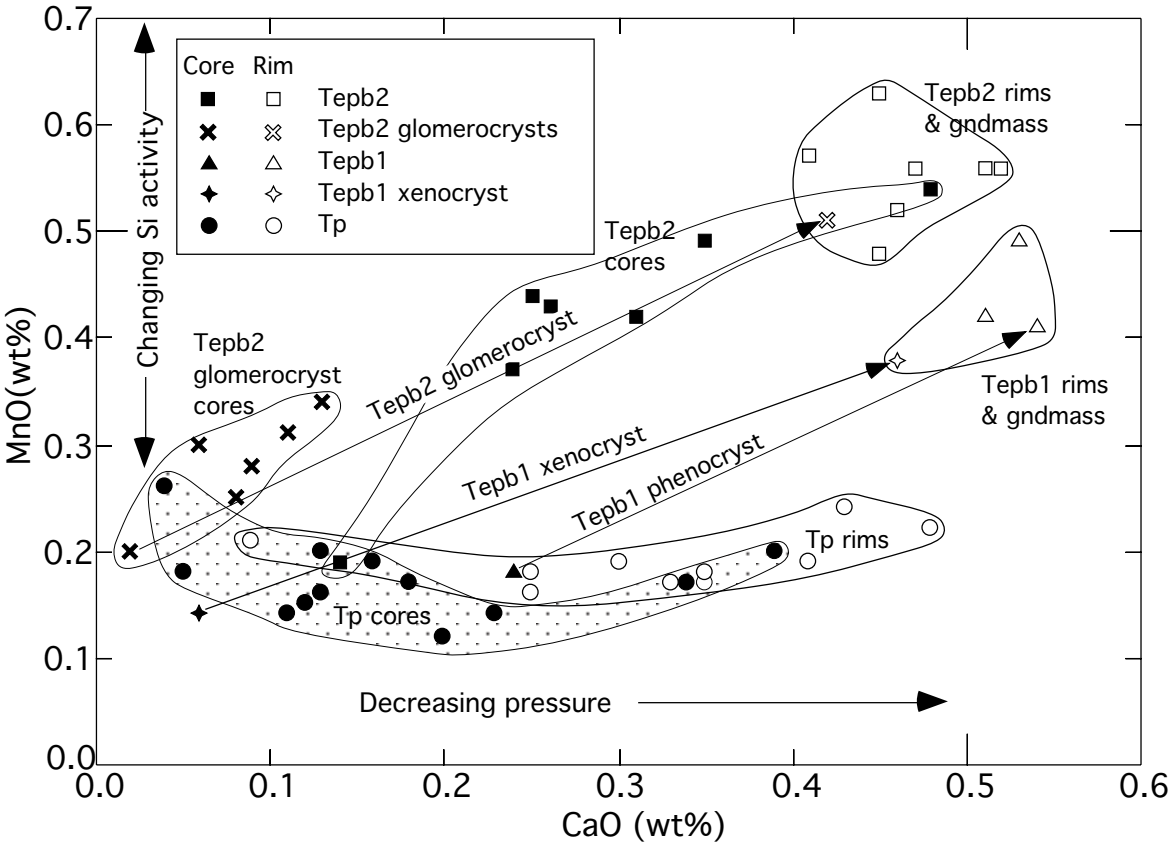

FIGURE 3. MnO *vs.* CaO concentrations in olivines, illustrating the effects of changing Si and Mn activities in the melt and decreasing pressure. The effect of decreasing pressure during crystallization is evident in all units. The "Tepb2" glomerocryst is interpreted to be xenocrystic, with crystallization conditions of the crystal cores similar to those of the "Tepb1" xenocryst and some "Tp" phenocryst cores. Crystal rims generally experienced similar (surface) pressure, but magma chemistries differed among the units. (See Figure 1 for explanation of unit symbols.)

Differences in MgO concentrations in tephra exposed at the NW and SE corners of Tejana Mesa suggest that there may be two tephras; nevertheless, we treat them as a single unit in this paper.

The compositions of early and late basanites overlap in SiO_2, alkalis, and $Fe_2O_3^t$ concentrations, but differ in MgO, Al_2O_3, and compatible trace elements (Fig. 4). The early basanite is chemically a true basanite; but the lower MgO concentration in late basanite causes it to vary from tephrite (normative ol < 10%) to basanite (normative ol > 10%) (LeMaitre, 1989). For simplicity, it is here referred to as basanite.

The higher Al_2O_3 content in late basanite corresponds to its more abundant aluminum-rich interstitial and veinlet silicate phases; and slightly greater TiO_2 concentration is reflected in higher Fe-Ti oxide abundance. The appearance of modal apatite corresponds to a very slight increase in P_2O_5. All these differences suggest that the late basanite is more chemically evolved than the early basanite, probably through increased olivine fractionation during late basanite evolution. (Because the SiO_2 content in olivine is similar to that in the basanites, forsteritic olivine fractionation would have little effect on the SiO_2 content of the basanites, would decrease MgO content, and would increase concentrations of most other elements.)

The most magnesian vein samples tend to lie on major element compositional trends defined by the basanites (Fig. 4). The alkali oxides and P_2O_5 concentrations are notable exceptions. Among the compatible trace elements, Cr and Ni concentrations show nearly identical patterns, dropping sharply with decreasing MgO in basanites and continuing to decrease with decreasing MgO concentration in veins. In contrast, V content closely mimics TiO_2.

Tephra and lava samples have similar incompatible element patterns, with nearly all analyzed elements being slightly more concentrated in lavas than in bombs. Veins tend to contain two to three times higher concentrations of incompatible elements than lavas (Fig. 5), consistent with the more evolved nature of vein magma. All samples are strongly depleted in Rb and K.

REE patterns in all rocks decrease from La to Lu, and contain no Eu anomalies (Fig. 6). The ratio La_N/Lu_N exceeds that of typical ocean island basalt, OIB, and is about equal to 50 in lavas and tephra, when the chondrite factors of Nakamura (1974) are used to normalize element concentrations.

One sample each from the early and late basanites have identical, within error, Nd isotopic compositions. Their present day ε_{Nd} is +3.2 (O. T. Rämö, personal commun., 1997).

Three whole rock $^{40}Ar/^{39}Ar$ ages, two on early basanite from the southeast corner of Tejana Mesa and one on late basanite from El Porticito, are, within error, identical, averaging 7.08 ± 0.25 Ma (2σ) (Table 4) (W. C. McIntosh, personal commun., 1996). A fourth sample, not shown in Figure 1, was taken from a dike ~500 m SSW of El Porticito. It yielded an age of 7.08 ± 0.64 Ma.

TABLE 2. Representative mineral compositions of volcanic rocks at El Porticito and Tejana Mesa.

Sample #	Rock/X'l	Composition	SiO_2	TiO_2	$Al2O_3$	FeO	Fe_2O_3	MnO	MgO	CaO	Na_2O	K_2O	P_2O_5	Total	Sr	Ba	Cr	V	Zn
Acc./Det. Lim.			1.5/ 0.3	0.7/ 0.4	0.7/ 0.2	1.1/ 0.5		0.3/ 0.3	0.4/ 0.2	0.5/ 0.2	0.3/ 0.1	0.8/ 0.1	0.04/ 0.1		1200/ 5800	1200/ 4100	6500/ 3700	700/ 1900	660/ 2500
	Tp:																		
21.1-36	micropheno.	Hem(Ilm45)	n.d.	22.9	1.5	18.5	54.0	0.8	0.7	n.d.	n.a.	n.a.	n.a.	98.8	n.a.	n.a.	n.d.	1900	n.d.
	Tepb1:																		
19A1-29	pheno. core	Cpx (En46)	52.1	1.1	2.6	3.1	1.0	n.d.	16.0	23.2	0.4	n.a.	n.a.	100.6	n.d.	n.a.	6600	n.a.	n.d.
19A1-109	gndmass.	Cpx (En41)	47.8	2.6	4.4	3.2	4.2	n.d.	13.9	22.5	0.6	n.a.	n.a.	99.4	n.a.	n.a.	n.d.	n.a.	n.d.
19A1-55	pheno. core	Ol (Fo90)	40.4	n.d.	n.d.	9.5		n.d.	49.8	n.d.	n.a.	n.a.	n.a.	100.4	n.a.	n.a.	n.d.	n.a.	n.d.
19A1-61	pheno. rim	Ol (Fo80)	38.8	n.d.	n.d.	18.1		0.4	42.7	0.5	n.a.	n.a.	n.a.	100.6	n.a.	n.a.	n.d.	n.a.	n.d.
19A1-19	gndmass.	Hem(Ilm24)	n.d.	15.9	1.9	6.8	70.4	0.6	3.7	n.d.	n.a.	n.a.	n.a.	101.8	n.a.	n.a.	11900	1900	n.d.
	Tepb2:																		
1B-162	pheno. core	Cpx (En45)	51.6	1.3	2.3	3.2	1.3	n.d.	16.0	23.3	0.3	n.a.	n.a.	99.8	n.a.	n.a.	n.d.	n.a.	n.d.
1B-165	pheno. rim	Cpx (En38)	45.8	3.7	7.1	5.1	2.3	n.d.	12.2	22.5	0.5	n.a.	n.a.	99.5	n.a.	n.a.	n.d.	n.a.	n.d.
1B-156	gndmass.	Cpx (En45)	50.6	1.3	2.5	2.5	2.9	n.d.	15.7	23.0	0.4	n.a.	n.a.	99.3	n.d.	n.a.	n.d.	n.a.	n.d.
6B-23	pheno. rim	Ol (Fo73)	37.8	n.d.	n.d.	23.3		0.5	37.8	0.4	n.a.	n.a.	n.a.	100.1	n.a.	n.a.	n.d.	n.a.	n.d.
	Tepv:																		
1B-146	pheno. core	Cpx (En39)	47.0	3.2	5.4	5.0	2.3	n.d.	12.7	22.5	0.5	n.a.	n.a.	98.8	n.a.	n.a.	n.d.	n.a.	n.d.
1B-149	pheno. rim	Cpx (En35)	43.7	4.7	8.2	4.9	3.2	n.d.	11.0	22.3	0.7	n.a.	n.a.	99.0	n.a.	n.a.	n.d.	n.a.	n.d.
5B-31	gndmass.	Cpx (En37)	43.7	4.5	7.9	3.9	3.8	n.d.	11.8	22.1	0.8	n.a.	n.a.	98.4	n.a.	n.a.	n.d.	n.a.	n.a.
1B-111	incl. in Cpx	Ne (Ne85.2)	48.8	n.d.	30.8	n.d.		n.a.	n.a.	1.2	16.0	2.3	n.d.	99.5	n.d.	n.d.	n.a.	n.a.	n.a.
1B-133	gndmass.	Fsp (Or28)	56.1	n.d.	22.8	0.5		n.a.	n.d.	2.4	5.0	4.3	n.d.	99.0	22330	46300	n.a.	n.a.	n.a.
15.1-40	gndmass.	Analcime	55.2	n.a.	23.4		0.2	n.a.	n.a.	n.d.	11.2	0.2	n.d.	90.5	n.d.	n.d.	n.a.	n.a.	n.a.
6B-41	gndmass.	Apatite	n.d.	n.d.	n.d.	n.d.		n.a.	n.d.	54.5	n.d.	n.d.	41.6	97.4	6400	n.d.	n.a.	n.a.	n.a.
1b-10	pheno. lam.	Mag (Usp4.9)	n.d.	1.6	7.1	26.8	58.6	2.2	2.6	n.d.	n.a.	n.a.	n.a.	99.8	n.a.	n.a.	n.d.	n.d.	3700

Major element concentrations in wt%.

Trace element concentrations in parts per million (ppm).

Iron in pyroxenes was partitioned between ferrous and ferric oxides using the method of Baldridge, 1979.

Iron in Fe-Ti oxides was partitioned between ferrous and ferric oxides using the method of Stormer, 1983.

Acc./Det. Lim.: Accuracy/Detection Limit, as determined from multiple analyses of in-house and industry standards.

Accuracy is defined as the average deviation from the accepted concentration plus 2 standard deviations.

Detection Limit is defined as the average concentration equivalent to the background noise plus 2 standard deviations.

For those samples in which Fe has been partitioned into ferrous and ferric oxides, Acc./Det. is stated for total iron as FeO.

n.a.: not analyzed.

n.d.: below detection limit.

TABLE 3. Major element compositions of volcanic rocks at El Porticito and Tejana Mesa.

			Tp		Tepb1			Tepb2			Tepv				
	s.d. / d.l.	a.m.	27C	49E	19A	29	55	37G	44F	56	15	25B	45A	45B	45C
SiO_2	0.38	XRF	39.93	41.63	42.05	42.55	42.11	41.93	41.33	42.87	43.50	41.91	47.91	48.34	44.30
TiO_2	0.01	XRF	2.78	2.67	2.90	2.98	2.92	3.14	3.13	3.15	3.26	3.38	2.12	2.09	3.14
Fe_2O_3	0.03	XRF	12.00	11.81	12.69	12.75	12.69	12.78	12.78	12.78	11.07	11.10	7.67	7.53	10.24
MnO	0.01	XRF	0.17	0.16	0.18	0.19	0.19	0.18	0.18	0.19	0.18	0.17	0.13	0.13	0.15
MgO	0.01	XRF	13.71	11.13	14.36	13.65	13.08	9.98	10.46	9.50	4.04	5.19	2.72	2.44	4.19
CaO	0.02	XRF	14.98	14.41	12.87	12.67	13.05	12.59	12.70	12.54	11.01	12.09	7.54	6.59	10.31
Na_2O	0.02	XRF	2.12	1.99	2.34	3.62	3.66	2.73	2.44	4.03	2.98	2.44	3.91	5.71	4.22
K_2O	0.04	XRF	0.35	0.56	1.00	0.49	0.59	0.88	0.82	0.93	2.95	2.20	3.74	3.89	2.97
P_2O_5	0.01	XRF	0.89	0.85	0.91	0.97	0.94	0.97	0.99	1.00	1.47	1.70	0.82	0.79	1.50
LOI	0.19	Grav	4.27	5.36	1.57	1.08	1.27	3.49	3.09	1.23	4.55	4.55	4.27	2.59	2.44
Total			99.61	99.19	99.67	100.05	99.58	99.81	98.69	99.48	100.28	98.73	98.78	98.76	98.87
V	1.4/1	XRF	226	274	250	249	260	250	267	283	200	268	90	84	220
Sc	0.017/0.01	INAA	23.2	22.3	24.1	24.1	23.9	19.4	20.3	19.8	5.1	8.5	1.7	1.3	5.1
Cr	0.05/0.01	INAA	708	684	710	697	672	363	390	367	3	32	5	2	3
Ni	0.8/0.1	XRF	433	414	391	389	385	218	232	233	33	52	26	16	54
Cu	16/2	XRF	82	69	84	73	80	120	100	98	181	181	109	119	150
Zn	1.6/1	XRF	115	113	107	106	110	110	107	116	111	98	84	87	103
Ga	2.5/2	XRF	15	15	17	19	18	21	20	21	18	20	21	23	22
As	0.6/0.1	XRF	3	19	1	3	4	3	6	4	6	8	13	9	7
Rb	1.6/1	XRF	13.0	52.4	16.5	15.6	6.4	57.5	22.4	17.0	96.5	44.1	75.6	82.1	58.0
Sr	2.3/1	XRF	1242	1016	1126	1070	1094	1168	1376	1228	2315	2119	4317	3357	2767
Y	2.2/1	XRF	24	23	25	26	25	27	28	29	33	36	27	29	36
Zr	5.7/2	XRF	239	231	248	256	254	264	259	274	320	332	314	326	326
Nb	1.6/1	XRF	74	70	72	74	74	77	73	83	122	125	156	162	121
Mo	55/2	XRF	2	0	0	2	1	1	1	2	3	3	1	3	2
Sb	5.0/2	INAA	n.d.	0.03	0.07	0.06	n.d.	0.05	0.09	0.04	n.d.	0.10	0.15	0.12	0.09
Cs	1.7/0.5	INAA	4.5	5.1	0.6	0.8	0.7	1.5	0.8	0.9	1.2	1.5	0.8	0.6	1.4
Ba	15/1	XRF	1040	1498	1300	1370	1342	1710	1662	1552	3108	2800	4896	4043	3014
La	1.2/2	INAA	72.7	69.8	74.9	78.6	78.2	81.9	82.5	84.2	128.0	137.0	121.3	123.5	127.5
Ce	1.0/2	INAA	141.0	132.9	143.3	150.4	148.9	156.0	158.3	160.8	237.2	253.4	211.4	216.6	232.9
Nd	3.6/2	INAA	55.3	53.7	56.9	66.0	59.5	65.6	64.7	61.4	88.0	100.5	82.5	76.7	97.5
Sm	1.3/1	INAA	11.1	10.7	11.8	11.8	12.6	12.1	13.1	12.5	15.7	17.2	12.2	12.3	16.3
Eu	1.0/1	INAA	3.1	3.0	3.3	3.4	3.3	3.4	3.5	3.5	4.3	4.8	3.5	3.6	4.4
Tb	1.8/0.5	INAA	1.1	1.1	1.2	1.2	1.2	1.2	1.2	1.2	1.4	1.6	1.1	1.2	1.5
Yb	1.1/1	INAA	1.5	1.4	1.5	1.5	1.4	1.8	1.6	1.7	2.3	2.3	2.0	2.2	2.2
Lu	1.4/0.1	INAA	0.2	0.2	0.2	0.2	0.2	0.2	0.2	0.2	0.3	0.3	0.2	0.3	0.3
Hf	1.4/1	INAA	5.7	5.6	6.1	5.9	6.1	6.3	6.5	6.5	6.3	6.9	5.9	5.7	6.9
Ta	1.3/1	INAA	4.1	4.0	4.2	4.4	4.4	4.8	4.5	4.8	7.8	8.0	8.8	9.1	7.4
Pb	1.7/1	XRF	6	6	8	6	8	8	7	8	14	11	16	15	13
Th	1.4/1	INAA	14.2	13.4	13.8	14.8	14.2	15.8	15.3	16.5	26.1	28.5	31.6	32.2	24.6

Major element components given in wt%; minor elements in ppm.

s.d. / d.l.: Estimated standard deviations / detection limits (ppm). Only s.d. is given for major elements.

For XRF measurements, 17 aliquots of in-house reference NMR were analysed to obtain the listed standard deviations.

For INAA measurements, 30 aliquots of BCR-1 and 33 aliquots of G-2 USGS standards were analysed.

For gravimetric measurements, 9 aliquots of sample 7A were analysed.

a.m..: analysis method

XRF: wavelength dispersive X-ray fluorescence

INAA: instrumental neutron activation analysis

Grav: gravimetric

n. d.: not detected

(This dike has major and trace element concentrations intermediate between those of veins and lavas at El Porticito and Tejana Mesa.)

DISCUSSION

Crustal Contamination

Colorado Plateau transition zone alkali basalts originate in the upper mantle (Perry et al., 1987), and must traverse continental crust en route to the surface, providing opportunities for contamination, with resultant enrichment in rare earth elements (REE) (Menzies et al., 1991) and large ion lithophile (LIL) elements, notably K and Rb (e.g. Reid et al., 1989). However, the tephra and lava trace element patterns of Figure 5 show depletion of K and Rb relative to other LIL elements, which implies that crustal contamination of these rocks was minimal.

Fractional crystallization and crustal contamination both result in decreased Mg-numbers (100 5 Mg/(Mg + Fe^{2+}) with Fe^{2+} =

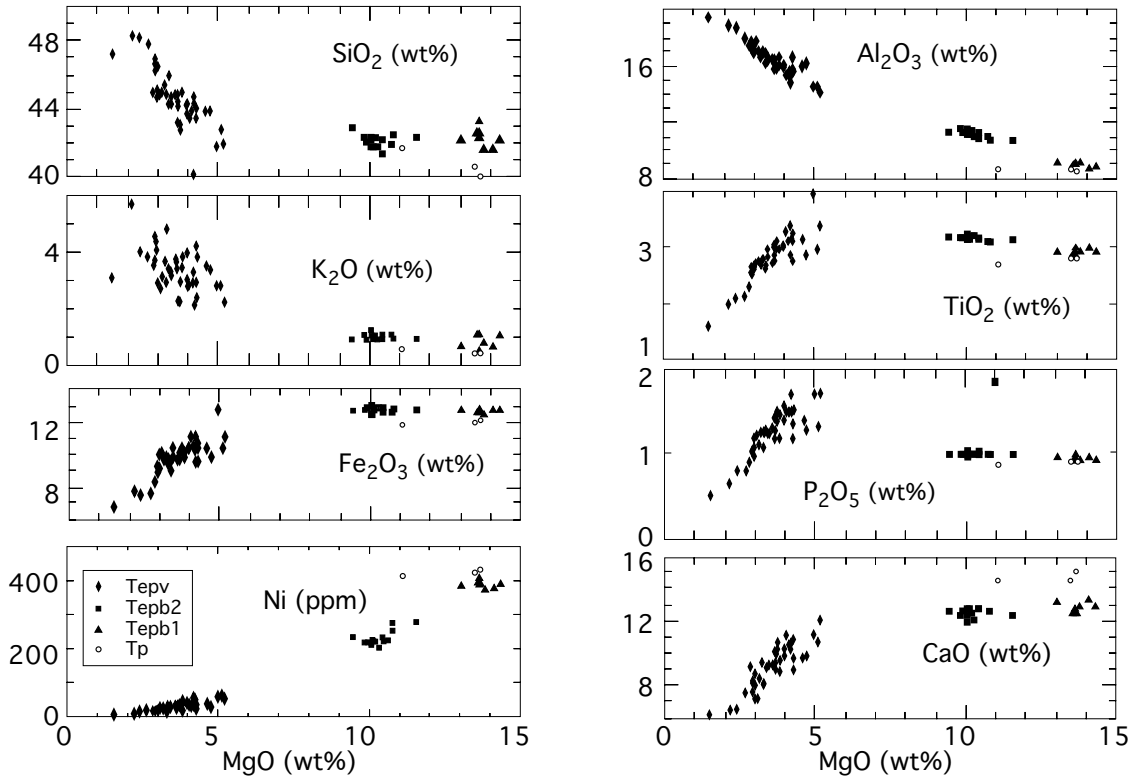

FIGURE 4. MgO variation diagrams for rocks found at El Porticito and Tejana Mesa. The rocks tended toward higher SiO_2, Al_2O_3, Ba, Sr and alkali concentrations and lower MgO, TiO_2, Fe_2O_3, Cr, Ni, and V concentrations as the eruptive sequence progressed. The high P_2O_5 concentration in many vein samples reflects the abundant apatite found in them.

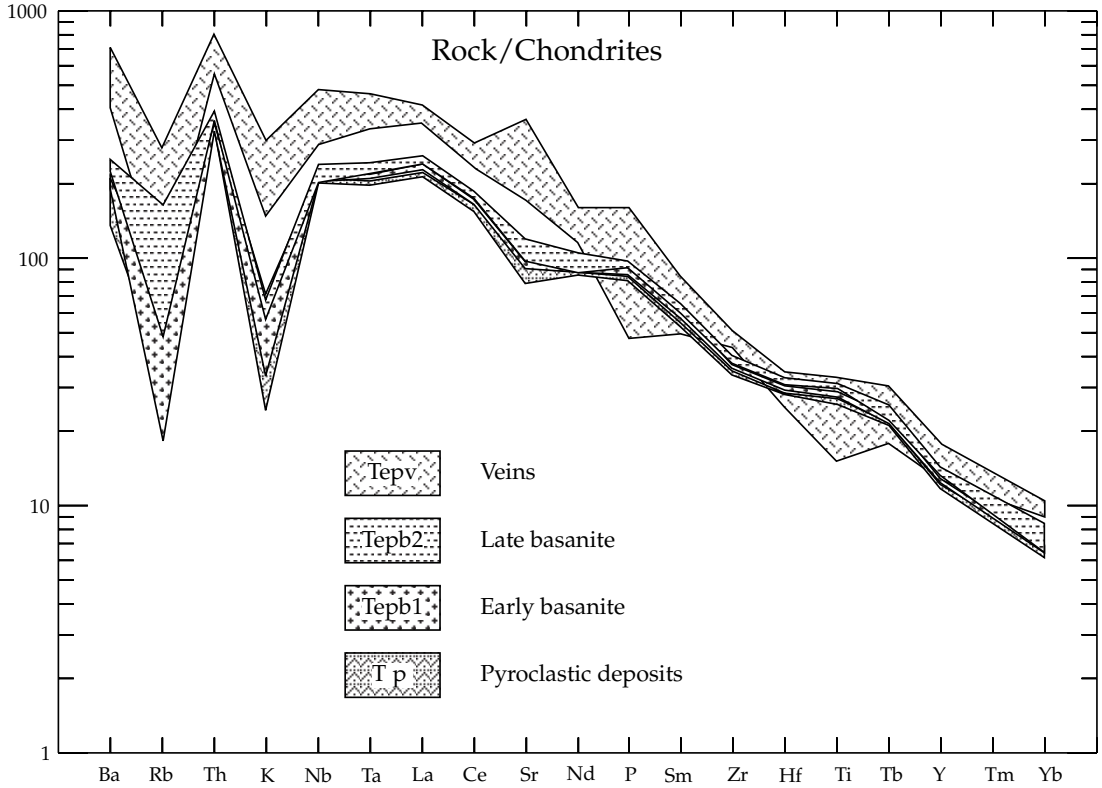

FIGURE 5. Chondrite-normalized incompatible trace element concentrations. Note the high concentrations of Ba and Th. These could indicate melting of lithospheric mantle enriched by fluids from a (Mazatzal accretion?) subducting slab. Enrichment of Nb, Ta, and LREE suggest further enrichment of lithosphere by melts resulting from low degree partial melting of the asthenosphere (lithosphere thinning associated with Rio Grande rifting?). The strong relative depletions of K and Rb suggest minimal involvement of continental crust during evolution of these rocks. (Normalization factors from Thompson, 1984.)

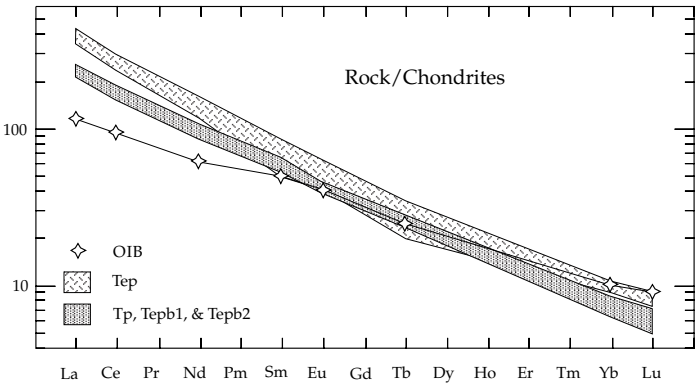

FIGURE 6. Chondrite-normalized rare earth element concentrations in volcanic rocks. LREE-HREE fractionation is stronger than typical ocean island basalts. This strong fractionation suggests a component of melt resulting from low degree partial melting of spinel (garnet?) lhertzolite. (OIB from Sun and McDonough, 1989; normalization factors from Nakamura, 1974.)

0.85 Fe^t). Nevertheless, basalts with Mg-numbers ≥68 "probably represent primary mantle magmas that were in equilibrium with upper mantle olivine compositions and subsequently erupted at the surface without significant compositional modification" (Perry et al., 1987). Within the study area, tephra and early basanite samples yield an average Mg-number of 72, suggesting little crustal contamination, while the average late basanite Mg-number is 65, perhaps due to slight crustal involvement or increased fractional crystallization.

The relatively high ε_{Nd} (+3.2) also suggests that crustal contamination, if any, was small. Thus, while assimilation of continental crust cannot be completely discounted, we conclude that it cannot have made a major contribution to most element concentrations in lava and tephra samples. These samples must be reasonably representative of mantle melts that have undergone some crystal fractionation prior to eruption.

Mantle Source

Neodymium isotopic data for both basanites yield ε_{Nd} = +3.2, suggesting derivation from a time-integrated depleted (relative to chondrites) mantle source. This isotopic composition is intermediate between "depleted" (asthenospheric) and "enriched" (lithospheric) mantle values, which have been estimated by Perry et al. (1987) as ~+8 for depleted mantle (DM) and ~+1 for enriched mantle (EM) and by Menzies et al. (1991) as ~+5 for DM and ~-4 for EM. (These estimates were for the Colorado Plateau-Basin and Range transition zone, and are not to be confused with the DM and EM's of Zindler and Hart, 1986.)

Tephra and basanites have high Ba_N, and Th_N (Fig. 5). Barium could be enriched by fluids from the lithosphere, itself enriched by fluids derived from a subducting slab (Tatsumi, 1989), since Ba tends to form highly water-soluble compounds. Thorium enrichment could result from either crustal contamination or involvement of a lithospheric mantle that had been enriched in Th by fluids emanating from the subducting slab associated with Mazatzal arc accretion (Menzies et al., 1991). Inasmuch as no evidence for crustal contamination exists, we associate high Ba and Th with a lithospheric mantle enriched by fluids from a subducting slab.

However, high Nb_N and Ta_N (Fig. 5) suggest that a subducting slab, in which these elements are usually retained during dehydration (McMillan, 1998), was not the only source of lithospheric mantle enrichment. Either very small partial melts derived from the convecting asthenosphere (McKenzie, 1989) or from mantle plumes (McMillan, 1998) could provide enrichment in Nb and Ta, as well as strong LREE-HREE fractionation (Fig. 6) (Wilson, 1989).

Taken together, these isotopic and trace element data suggest an enriched lithospheric mantle source with composition inter-

TABLE 4. Summary of whole rock $^{40}Ar/^{39}Ar$ age determinations.

Sample	Location ‡	Unit	Analysis	n	40/36	Err	Age	±2 sigma	Comments
28	Tejana Mesa 0723720E 3807880N	Tepb1	isochron	7	296.9	2.9	7.13	0.30	b-g steps
29	Tejana Mesa 0723740E 3807920N	Tepb1	step H	1			6.94	0.34	61.1% ^{39}Ar in H step
6B	El Porticito 0723430E 3807950N	Tepb2	isochron	9	300.4	1.2	7.17	0.70	all steps, low yields
mean age							7.08	0.25	
32	* 0723000E 3807200N	Dike	isochron	7	297.6	1.8	7.08	0.64	b-h steps

‡ Sample coordinates are referenced to UTM Zone 12, 1927 North American datum. Estimated accuracy is ±10 m, except sample 32, for which the estimated accuracy is ± 100 m.

* This sample was taken from a basanite dike located ~500 m SSW of the study area.

$^{40}Ar/^{39}Ar$ dating (Dalrymple et al., 1981, and McDougall & Harrison, 1988) of samples was performed at the New Mexico Geochronology Research Laboratory at NMT, using a MAP 215-50 mass spectrometer, operated in electron multiplier mode, to determine relative isotopic abundances.

TABLE 5. Least-squares fractional crystallization mass balance solutions for tephrites and basanites.

	SiO_2	TiO_2	Al_2O_3	FeO	MnO	MgO	CaO	Na_2O	K_2O	P_2O_5	ΣR^2
	Tepb⇒Tepv										
Add analyzed minerals to Tepv (sample 25B) to obtain Tepb2 (sample 44F):											
44F = 0.441 (25B) + 0.319 Cpx(En_{39}) + 0.119 Ol(Fo_{73}) + 0.032 Hem(Ilm_{45}) + 0.005 Ap + 0.086 Ne($Ne_{85.2}$)											
meas	43.82	3.32	11.43	12.20	0.19	11.08	13.46	2.58	0.87	1.05	
calc	43.79	3.42	11.11	12.17	0.23	11.10	13.47	2.70	1.24	1.04	0.187
weight	0.4	1.0	0.5	1.0	1.0	1.0	1.0	1.0	1.0	1.0	
	Tepb1⇒Tepv										
Add analyzed minerals to Tepv (sample 25B) to obtain Tepb1 (sample 19A):											
19A = 0.316 (25B) + 0.381 Cpx(En_{41}) + 0.181 Ol(Fo_{80}) + 0.033 Hem(Ilm_{45}) + 0.008 Ap + 0.081 Ne($Ne_{85.2}$)											
meas	43.43	3.00	9.09	11.79	0.18	14.83	13.29	2.42	1.03	0.94	
calc	43.33	2.96	9.18	11.80	0.19	14.84	13.32	2.41	1.07	0.91	0.010
weight	0.4	1.0	0.5	1.0	1.0	1.0	1.0	1.0	1.0	1.0	
	Tepb1⇒Tepb2										
Add analyzed minerals to Tepb2 (sample 44F) to obtain Tepb1 (sample 19A):											
19A = 0.631 (44F) + 0.189 Cpx(En_{46}) + 0.096 Ol(Fo_{90}) + 0.032 Hem(Ilm_{45}) + 0.007 Ap + 0.044 Ne($Ne_{85.2}$)											
meas	43.43	3.00	9.09	11.79	0.18	14.83	13.29	2.42	1.03	0.94	
calc	43.42	3.10	9.20	11.76	0.17	14.84	13.29	2.44	0.73	0.95	0.107
weight	0.4	1.0	0.5	1.0	1.0	1.0	1.0	1.0	1.0	1.0	

The residuals for Tepb2⇒Tepv and Tepb1⇒Tepb2 are an order of magnitude larger than for Tepb1⇒Tepv. Therefore, we infer that Tepv probably evolved from Tepb1 but that Tepb2 did not evolve from Tepb1. The weighting factors for SiO_2 and Al_2O_3 were arbitralily set less than 1 in order to emphasize somewhat the influence of other oxides on the residules. "Hem" crystals are members of the solid solution series hematite/ilmenite, and are considered to be magmatic. Both nepheline, "Ne" and hematite crystals, although listed as groundmass phases in Table 2, are partially enclosed by phenocrysts. Therefore, we consider them to be capable of participating in crystal fractionation. For further details, see Horning, 1997.

mediate between EM and DM, or some mix of materials from the two, as in the "plum pudding" model of Perry et al. (1987). This source is enriched in LIL elements (except K and Rb) and LREE but has a time-integrated, depleted isotopic signature. Lithosphere enrichment probably resulted from both low degree asthenospheric partial melts and subducting slab fluids.

Lava and Vein Petrogenesis

The trends in whole rock composition evident for most elements shown in Figure 4 strongly suggest that the most mafic vein samples evolved from late basanite, which in turn evolved from early basanite. Oxides of potassium and phosphorous are notable exceptions. The location of veins in late basanite reinforces the suggestion that veins derived from late basanite. In order to test this hypothesis, we have conducted least squares mass balance numerical modeling of major element compositions (Bryan et al., 1969; Stormer and Nicholls, 1978). This modeling utilized the chemical compositions of mineralogical assemblages observed in both parent and daughter rocks. Vein samples exhibit a wide range of compositions; and we have chosen the most mafic vein sample in order to minimize the effects of evolution evident within veins. Table 5 summarizes the best effort results. Although all residuals are small, and therefore somewhat ambiguous, they suggest that the two lavas evolved independently from the common mantle source described above, and that vein magma evolved from early, not late, basanite.

Model trace element concentrations, based upon measured whole rock compositions and published mineral-melt partition coefficients, support these conclusions. In particular, the differences between calculated and observed concentrations of Cr and Ni, assuming fractionation of the most mafic vein samples from early basanite, are 20 to 50 times smaller than for assumed fractionation from late basanite. Attempts to calculate compatible trace element concentrations in late basanite, assuming fractionation from early basanite, were also unsuccessful.

We conclude that the data support the distinct evolutions of early and late basanites from a common parent and the fractionation of vein magma from the early basanite. We recognize, however, that the results of geochemical modeling are not unequivocal, and that the solutions of the two vein-generation models are not robust enough, or dramatically different enough, to rule out

fractionation of the vein magma from the earlier basanite. However, as fractionation from the early basanite represents a better modelled fit, this will be our leading hypothesis.

Age

Both the earlier (McIntosh and Cather, 1994) $^{40}Ar/^{39}Ar$ and present age determinations were accomplished in the New Mexico Geochronology Research Laboratory at New Mexico Tech (NMT). The present value, 7.08 ± 0.25 Ma, is considered to supercede the earlier determination, 7.92 ± 0.40 Ma (W. C. McIntosh, personal commun., 1996).

Emplacement Model

The nature of the study area's magmatic plumbing is problematic. Guilinger (1982) and Baldridge et al. (1989) suggested that El Porticito and the immediately adjacent Tejana Mesa might represent a lava lake. The near vertical original contact orientation between early and late basanites at El Porticito; the existence of the tilted basalt of Tejana Mesa flow in the volcanic stack at Tejana Mesa; and the repetition of late basanite in that stack seem to preclude this simple interpretation. The existence of wall rock fragments, some still partially attached to the walls, suggests that veins were forcefully emplaced. This evidently precludes the extraction of vein magma from host rock at the levels now exposed. Instead, vein magma ascended from depth.

Several other physical models might be proposed. One of these is a zoned chamber in which all tephra and magmas evolved and from which they erupted. We infer from Ca concentrations in olivine and from our geochemical modeling that this is unlikely, but certainly not impossible.

Figure 7 illustrates two other possibilities. These differ in the basanite from which vein magma evolved. Each includes two magma chambers for the separate evolution of the two basanites. Both chambers were probably zoned. The chambers may be part of a complex arrangement of conduits similar to that beneath Kilauea, Hawaii (Decker, 1987; Philpotts, 1990, fig. 4-5). The depths of these chambers are unknown. However, the distinct CaO contents of the least calcic late basanite olivine phenocryst core (CaO =0.14 wt%) and the early basanite phenocryst core (CaO = 0.24 wt%) (Fig. 3) suggest (Stormer, 1973) that early basanite started crystallizing at a shallower depth than late basanite. We have not calculated the depths of these chambers because the Ca concentrations are essentially at the detection limit of the measurement equipment. Furthermore, crystallization temperature is required in most geobarometer calculations, but no minerals that are suitable for geothermometer calculations are available in our samples.

The pyroclastic deposits resulted from magmatic and phreatomagmatic eruptions from one or both these chambers. These eruptions are interpreted to have formed a maar-like depression and tuff ring. Exposed tephra suggests that this tuff ring had a width of about 600 m and depth of at least 60 m (Fig. 1). The maximum horizontal and vertical dimensions are not well constrained; and the total exposed thickness of lavas at El Porticito and Tejana Mesa exceeds 100 m, suggesting that the depression

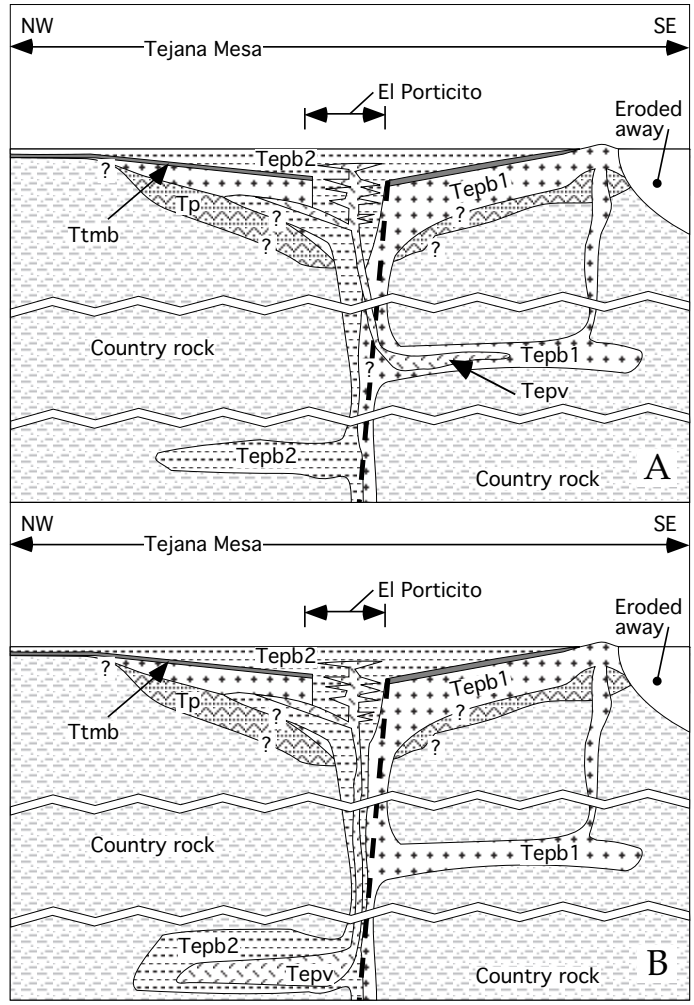

FIGURE 7. Cartoon illustrating volcanic evolution and emplacement models. Order of events was emplacement of tephra (Tp), older basanite (Tepb1), and lava of unknown origin (Ttmb); movement on the fault seen on the south face of Tejana Mesa to form a paleovalley; and finally emplacement of younger basanite (Tepb2) and veins (Tepv). The principal volcanic conduit may have coincided with the fault. Early basanite also erupted through a vent to the SE. Geochemical modeling suggests that basanites evolved independently from a common lithosphere-derived parent. A. Modeling also indicates that vein magma probably evolved from early basanite, then migrated within the principal conduit into hotter, weaker late basanite. B. Alternatively, if vein magma evolved at depth from late basanite, then there is no requirement for migration from one basanite into the other. (No vertical or horizontal scales.)

into which lavas flowed was considerably deeper than the thickness of exposed tephra. The tuff ring lies along a trend of volcanic vents, and may be the surface expression of a feeder dike beneath them (R. M. Chamberlin, personal commun. 2003).

Major and trace element differences between bombs found at the NW and SE corners of Tejana Mesa (Fig. 1) may indicate that both chambers, each with its own evolving composition, were sources for the two deposits. However, the continuum of olivine phenocryst compositions in tephra (Fig. 3), could be consistent with there being a single, zoned magma chamber (R. M. Chamberlin, personal commun. 2003). In any case, we have grouped all

tephras together as a single stratigraphic unit. Their proximity to El Porticito suggests that it probably was the location of the vent for one or both the deposits.

Early basanite lava overlies the tuff ring deposits. We infer that El Porticito was the source of this eruption. A separate flow with early basanite composition crops out at the SE corner of Tejana Mesa (Fig. 1). The portion of this unit that has vertical contacts is interpreted to have occupied a fissure through which a portion of early basanite erupted (Fig. 7).

Basalt of Tejana Mesa, erupted from an unknown vent, flowed over most of the presently-exposed early basanite at Tejana Mesa. However none of this basalt has been observed overlying the early basanite flow at the SE corner of Tejana Mesa, and the latter may have formed a topographic high at that location. Whether basalt of Tejana Mesa ever covered El Porticito is unknown. Movement along a fault (formerly mapped as the Mesa Tinaja fault (Chamberlin, et al., 1994)), resulted in rotation of beds and formation of a paleovalley on the upper surface of the basalt of Tejana Mesa. This valley may have been the surface expression of a shallow magma chamber's foundering roof.

Into this paleovalley flowed late basanite. The near-vertical contact, with no indication of faulting or erosion, between the two basanites at El Porticito is taken to indicate that late basanite erupted through, or beside, early basanite at that location. Therefore, we assume that El Porticito was the vent for the late basanite flow atop Tejana Mesa. Late basanite also intruded beneath, or into, early basanite NW of the above-mentioned fault at Tejana Mesa. The indistinct contacts between the intruded basanites at both El Porticito and Tejana Mesa probably indicates that early basanite was still hot enough to be, or become, plastic near the contact during the intrusion. Such indistinct, plastic, contacts have been observed at the lower contact of the lowest and thickest intrusive sheet of the Holyoke flood basalt in the Hartford Basin, Connecticut (Philpotts et al., 1996).

Because the lower contact of the late basanite intrusion at Tejana Mesa is everywhere covered, its precise nature is uncertain. Late basanite may have intruded early basanite; or possibly late basanite invaded poorly consolidated tephra underlying early basanite. No basal flow breccia or lower vesicular zone (Aubele, et al., 1988) remains in early basanite at this location. Such structures would be expected near the bottom of a flow, and are observed elsewhere in early basanite where its base is clearly exposed. Thus it appears more likely that late basanite intruded the early basanite itself, as it did at El Porticito.

Geochemical modeling suggests that late basanite probably did not evolve from early basanite, and therefore represents a separate magma pulse. Although viscosity and/or density contrasts might have prevented mixing of the two magmas if late basanite erupted through an evolving early basanite chamber (or through overlying early basanite in a single, zoned chamber or lava lake) their similar compositions and grain sizes, and the probable high temperature of the early basanite chamber at late basanite eruption time, suggest that their densities and viscosities probably were also similar, so that mixing would have occurred had the magmas mingled. This seems to favor a geometry in which the late basanite conduit bypasses the early basanite chamber. Furthermore, if vein magma evolved from early basanite, any late basanite pulse could not have significantly disturbed the chamber in which that evolution was progressing. Otherwise, veins would have different compositions than now observed.

Vein melt segregation may have been accomplished by filter pressing. The low number density of coarse augite phenocrysts found in veins, compared to augite crystals in early basanite, suggests that augite nuclei were removed from vein magma by porous flow (Philpotts et al., 1996) or fusion (Puffer and Horter, 1993) during ascent. This resulted in random, low concentrations of nuclei in vein melt, and probably accounts for the varied compositions found in vein samples.

If vein magma did in fact evolve from the early basanite, it had to find its way out of that basanite and into late basanite below exposures now seen in the study area. In Figure 7a, vein magma initially followed the same path as early basanite, but then migrated into the younger, hotter, and more fluid late basanite. Alternatively, vein magma might have risen through fractures in country rock into overlying lavas, not following the existing conduit at all. However, if that were the case, an explanation of why veins are not seen in early basanite, except for those few associated with the tephrite sill at Tejana Mesa, is required. In Figure 7b, vein magma evolved from the late basanite; there was no need for vein melt to migrate into a host different from its origen.

At the levels now exposed, the ascending vein melt was injected into a solidifying late basanite magma mush. Shrinkage of the mush, and/or foundering of solidifying upper crust, may have aided the process by providing room for vein melt (Marsh et al., 1991). Intrusion must have been forceful, as indicated by the fragments of wall rock found in veins, some apparently in the process of being detached when the veins solidified. The intrusive nature of veins implies that strong deviatoric stresses existed, forcing vein magma upward. The cause of these stresses is unknown, but the basalt of Tejana Mesa paleovalley into which late basanite flowed existed at vein intrusion time. Further collapse of a shallow magma chamber roof, similar to that which may have created the paleovalley, or movement along the fault now seen in the face of Tejana Mesa may have triggered vein emplacement and also ruptured or weakened the late basanite crystal mush, just as it was becoming brittle. Alternatively, differential stresses caused by crystal mush compaction in a shallow early basanite chamber, or rise of another pulse of melt from below, may have forced vein magma upward. These possibilities are not mutually exclusive.

Probably the late basanite body at El Porticito was hotter in its interior than near its margins at the time of vein intrusion, resulting in lower crystallinity and viscosity in the interior than near the margins. Smoothly curved veins suggest that deformation in response to the intrusion, perhaps near the center, was largely ductile; but abrupt, angular changes in vein orientation at the NW corner of El Porticito suggest intrusion into brittle fractures, perhaps near the margin. Since the late basanite appears to exhibit both ductile and brittle deformation, it must have been cooling through the rheological critical melt percentage (Arzi, 1978), or critical melt fraction (van der Molen and Paterson, 1979), at vein intrusion time. Local vein intrusion into overlying early basanite

at Tejana Mesa along relatively smoothly varying trajectories strengthens the conclusion that this basanite probably also varied some in temperature and locally possessed, or developed, some ductility at the time of vein emplacement.

Once in place, vein magma cooled rapidly, as indicated by the skeletal and spherulitic groundmass feldspar morphologies, typical of strongly supercooled conditions (Lofgren, 1980). The relatively small number of large pyroxene and Fe-Ti oxide phenocrysts suggests that the number density of these nuclei was low. But the concentrations of elements that compose these phases were high, so cooling produced large crystals. There were also sufficient components to produce abundant small phenocrysts that inhomogeneously nucleated and grew on wall rock. That most small, wedge-shaped pyroxene crystals remain attached to the wall rock on which they nucleated, and that large phenocrysts, although broken, very seldom have fragments displaced from one another, indicates that most pyroxene growth occurred after essentially all vein magma flow had ceased.

In analogy with the cooling behavior of the 1959 Kilauea Iki lava lake (Helz, et al., 1989), the ~30 m thick early basanite flow at Tejana Mesa probably would have solidified in about a decade had it not been intruded and covered by late basanite. Emplacement of late basanite undoubtedly slowed cooling of early basanite; nevertheless we estimate that the elapsed time between emplacements of early basanite and veins was probably just a few decades. This short interval is within the estimated uncertainty of whole rock $^{40}Ar/^{39}Ar$ dating, ±0.25 Ma (2σ), and is consistent with the absence of field evidence for significant temporal breaks.

A satisfactory explanation for the formation of the submillimeter, alkali feldspar and analcime rich veinlets found throughout late basanite intrusions remains problematic. The consistent horizontal orientation of veinlets indicates that the least principal stress was vertical, and possibly negative, at the time of their formation. Furthermore, the range of veinlet thickness, on the order of 50 to 200 μm, appears to be consistent throughout the intruded late basanite outcrops (except perhaps near the very top of El Porticito). It is not clear whether all veinlets formed simultaneously. However, uniform veinlet thicknesses suggest that mechanical properties in the volume of late basanite in which veinlets formed at any instant were consistent. At El Porticito itself, this uniformity extended vertically at least 60 m. Marsh et al. (1991), citing Moore and Evans (1967) and Wright and Okamura (1977), suggested that thermal contraction of solidifying magma might have been the mechanism that created space for segregation veins in Hawaiian lava lakes. This mechanism may have been operative in the formation of veinlets in the late basanite, but it remains unclear why veinlets are consistently horizontal. Evidently veinlet formation did depend upon the partially molten nature of the late basanite, since no veinlets have been observed in early basanite, which was probably solid, although locally plastic, at vein intrusion time. That they merge smoothly into both vein and host groundmasses, mineralogically and texturally, supports the conclusion that veinlets formed while both veins and host rock contained liquid magmatic phases.

Vein Color

The single, most eye-catching feature of El Porticito and adjacent Tejana Mesa is the coarse-grained, leucocratic veins set in melanocratic host. Why are the colors of these two rocks so different, although they are all mafic? The answer appears to lie in the details of chemical composition and resulting mineralogies.

The concentrations of those elements likely to impart dark color to a rock differ substantially in the two units. The MgO concentration in veins is less than or equal to about half that in late basanite; and TiO_2 and total iron concentrations in veins average about three quarters those in late basanite. Chrome and Ni are both important trace elements in lavas, but not in veins (Fig. 4). These compositional distinctions between basanites and veins led to major mineralogical differences. In late basanite the dominant minerals are titanaugite (~55-80%) and iron-titanium oxides (~10-25%). Leucocratic minerals comprise a minor portion of the groundmass, and are non-existent as phenocrysts. By contrast, veins are dominated by groundmass leucocratic phases: feldspar, analcime, leucite, zeolites, and sericite, which together comprise ~45-90% of the rock. Titanaugite and Fe-Ti oxide phenocrysts, while notable in hand specimen and thin section, typically occupy considerably less than half the rock surface.

CONCLUSIONS

Two chemically distinct black basanite lavas and white tephrite-phonotephrite veins, all emplaced at 7.08 ± 0.25 Ma, form El Porticito and most of the immediately adjacent Tejana Mesa. The two basanites derived from a common mantle source, apparently at the same time and in close proximity. The eruptive sequence began with the formation of a tuff ring, whose vent is inferred to be El Porticito. Into this tuff ring flowed the first, less-evolved basanite. After emplacement of minor-volume lava of unknown origin atop the first basanite, faulting created a paleovalley into which erupted the second basanite. This second, more-evolved basanite erupted through the first at El Porticito and also intruded the first basanite at Tejana Mesa.

The melt that formed the white veins fractionated at an unknown depth from magma more likely similar to the first basanite than the second. Vein melt carried pyroxene and Fe-Ti oxide crystal nuclei, now represented by coarse phenocrysts in the central portions of veins, through ruptures in the second basanite's crystallizing magma residing in the El Porticito conduit, stopping when it reached the upper rigid crust (Marsh et al., 1991). Thus, unlike veins found in other mafic bodies (e.g. Shonkin Sag laccolith (Osborne and Roberts, 1931), Kilauea Iki lava lake (Helz et al., 1989)), and flood basalts of the Hartford Basin (Philpotts et al., 1996), the veins of El Porticito apparently evolved from a parent of different composition from the host in which they were emplaced. There was little or no mixing of vein and host magmas during vein emplacement, probably because of the large viscosity contrast between the magmas.

The salient feature at El Porticito is the distinct origins of veins and their host rock; each derived from separate, identifiable, pulses of magma that evolved from the mantle. The color of

the veins, controlled by chemical and mineral composition, and the occurrence of their intrusion just as their host reached critical crystallinity, created the unique appearance of El Porticito.

ACKNOWLEDGMENTS

The authors wish to thank J. M. Farren, D. P. Miggins, and W. B. Vandermolen for invaluable assistance in the field; M. G. Snow for extensive help with the electron microprobe at the Los Alamos National Laboratory; W. C. McIntosh, L. Peters and R. P. Esser, of the New Mexico Geochronology Research Laboratory at NMT for $^{40}Ar/^{39}Ar$ dating; C. G. McKee for assistance in the X-ray Fluorescence laboratory at NMT; and O. T. Rämö of the University of Helsinki for $^{143}Nd/^{144}Nd$ analyses. K. Panter provided assistance in mass balance modeling. Special thanks are due N. G. Baca for allowing access to the study area. The authors wish to thank R. M. Chamberlin and N. J. McMillan for helpful reviews of this paper. The XRF lab at NMT was partially funded by NSF grant (EAR93-16467). The New Mexico Bureau of Geology and Mineral Resources provided partial funding, which is greatly appreciated, for this study.

REFERENCES

Aldrich, M. J., Jr. and Laughlin, A. W., 1984, A model for the tectonic development of the southeastern Colorado Plateau boundary: Journal of Geophysical Research, v. 89, p. 10,207-10,218.

Arzi, A. A., 1978, Critical phenomena in the rheology of partially melted rocks: Tectonophysics, v. 44, p. 173-184.

Aubele, J. C., Crumpler, L. S. and Elston, W. E., 1988, Vesicle zonation and vertical structure of basalt flows: Journal of Volcanology and Geothermal Research, v. 35, p. 349-374.

Baldridge, W. S., 1979, Mafic and ultramafic inclusion suites from the Rio Grande rift (New Mexico) and their bearing on the composition and thermal state of the lithosphere: Journal of Volcanology and Geothermal Research, v. 6, p. 319-351.

Baldridge, W. S., 1994, Petrographic summary of Late Miocene volcanic rocks of El Porticito: New Mexico Geological Society, 45th Field Conference, Guidebook, p. 61.

Baldridge, W. S., Perry, F. V., Nealey, L. D., Laughlin, A. W. and Wohletz, K. H., 1989, Field guide to excursion 8A: Oligocene to Holocene magmatism and extensional tectonics, central Rio Grande rift and southeastern Colorado Plateau, New Mexico and Arizona, *in* Chapin, C. E. and Zidek, J., eds., Field Excursions to Volcanic Terranes in the Western United States, Volume I: Southern Rocky Mountain Region: Socorro, New Mexico Bureau of Geology and Mineral Resources, Memoir 46, p. 219-221.

Baldridge, W. S., Perry, F. V., Vaniman, D. T., Nealey, L. D., Leavy, B. D., Laughlin, A. W., Kyle, P., Bartov, Y., Steinitz, G., and Gladney, E. S., 1991, Middle to late Cenozoic magmatism of the southeastern Colorado Plateau asnd central Rio Grande Rift (New Mexico and Arizona, U.S.A.): a model for continental rifting: Tectonophysics, v. 197, p. 327-354.

Barksdale, J. D., 1937, The Shonkin Sag laccolith: American Journal of Science, v. 33, p. 321-359.

Barksdale, J. D., 1952, The pegmatite layer in the Shonkin Sag laccolith, Montana: American Journal of Science, v. 250, p. 705-720.

Bryan, W. B., Finger, L. W. and Chayes, F., 1969, Estimating proportions in petrographic mixing equations by least-squares approximation: Science, v. 163, p. 926-927.

Cas, R. A. F. and Wright, J. V., 1993, Volcanic Successions Modern and Ancient: London, Chapman and Hall, 528 p.

Chamberlin, R. M., Cather, S. M., Anderson, O. J. and Jones, G. E., 1994, Reconnaissance geologic map of the Quemado 30 5 60 minute quadrangle, Catron County, New Mexico: New Mexico Bureau of Geology and Mineral Resources, Open-File Report 406, 29 p.

Chapin, C. E., Chamberlin, R. M., Osborn, G. R., Sanford, A. R. and White, D. W., 1978, Exploration framework of the Socorro geothermal area, New Mexico, *in* Chapin, C. E. and Elston, W. E., eds., Field Guide to Selected Cauldrons and Mining Districts of the Datil-Mogollon Volcanic Field New Mexico: Socorro, New Mexico Geological Society Special Publication No. 7, p. 114-129.

Dalrymple, G. B., Alexander, E. C., Lanphere, M. A. and Kraker, G. P., 1981, Irradiation of samples for $^{40}Ar/^{39}Ar$ dating using the Geological Survey TRIGA reactor: U. S. Geological Survey Professional Paper 1176.

Decker, R. W., 1987, Dynamics of Hawaiian volcanoes: an overview, *in* Decker, R. W., Wright, T. L. and Stauffer, P. H., eds. Volcanism in Hawaii: Washington, D.C., U. S. Geological Survey Professional Paper 1350, p. 1395-1447.

Dethier, D. P., Aldrich, M. J., Jr. and Shafiqullah, M., 1986, New K-Ar ages for Miocene volcanic rocks from the northeastern Jemez Mountains and Tejana Mesa, New Mexico: Socorro, New Mexico Bureau of Mines and Mineral Resources, and Reno, Nevada Bureau of Mines and Geology, Isochron/West, v. 47, p. 12-14.

Guilinger, D. R., 1982, Geology and Uranium Potential of the Tejana Mesa-Hubbell Draw area, Catron County, New Mexico [M. S. thesis]: Socorro, New Mexico Institute of Mining and Technology, 129 p.

Hallett, R. B. and Kyle, P. R., 1993, XRF and INAA determinations of major and trace elements in Geological Survey of Japan igneous and sedimentary rock standards: Geostandards Newsletter, v. 17, p. 127-133.

Hamilton, W., Hayes, P. T., Calvert, R., Smith, V. C., Elmore, P. S. D., Barnett, P. R. and Conklin, N., 1965, Diabase Sheets of the Taylor Glacier Region Victoria Land, Antarctica: Washington, D.C., U. S. Geological Survey Professional Paper 456-B, 71 p.

Helz, R. T., Kirschenbaum, H., and Marinenko, J. W., 1989, Diapiric transfer of melt in Kilauea Iki lava lake, Hawaii: A quick, efficient process of igneous differentiation: Geological Society of America Bulletin, v. 101, p. 578-594.

Horning, R. R., 1997, Field relationships and evolution of leucocratic, basic veins at El Porticito volcanic vent, New Mexico [M. S. thesis]: Socorro, New Mexico Institute of Mining and Technology, 146 p.

Hurlbut, C. S. and Griggs, D. T., 1939, Igneous rocks of the Highwood Mountains, Montana: Part I. The Laccoliths: Geological Society of America Bulletin, v. 50, p. 1043-1112.

Karlstrom, K. E. and Bowring, S. A., 1993, Proterozoic orogenic history of Arizona, *in* Van Schmus, R. A. and Bickford, M. E., eds., Precambrian Coterminous United States. Geology of North America: Boulder, Geological Society of America, v. C-2, p. 188-211.

Karlstrom, K. E. and Daniel, C. G., 1993, Restoration of Laramide right-lateral strike slip in northern New Mexico by using Proterozoic piercing points: Tectonic implications from the Proterozoic to the Cenozoic: Geology, v. 21, p. 1139-1142.

LeMaitre, R. W., 1989, A Classification of Igneous Rocks and Glossary of Terms: Oxford, Blackwell Scientific Publications, 191 p.

Lofgren, G. E., 1980, Experimental studies on the dynamic crystallization of silicate melts, *in* Hargraves, R. B., ed., Physics of Magmatic Processes: Princeton, Princeton University Press, p. 487-551.

Luttinen, A. V., Rämö, O. T., and Huhma, H., 1998, Neodymium and strontium isotopic and trace element composition of a Mesozoic CFB suite from Dronning Maud Land, Antarctica: Implications for lithosphere and asthenosphere contributions to Karoo magmatism, Geochimica et Cosmochimica Acta, v. 62, p. 2701-2714.

Mahood, G. A. and Cornejo, P. C., 1992, Evidence for ascent of differentiated liquids in a silicic magma chamber found in a granitic pluton: Transactions of the Royal Society of Edinburgh: Earth Sciences, v. 83, p. 63-69.

Marsh, B. D., Gunnarsson, B. Congdon, R. and Carmody, R., 1991, Hawaiian basalt and Icelandic rhyolite: indicators of differentiation and partial melting: Geologische Rundschau, v. 80/2, p. 481-510.

McDougall, I. and Harrison, T. M., 1988, Geochronology and Thermochronology by the $^{40}Ar/^{39}Ar$ method: London, Oxford University Press.

McIntosh, W. C. and Cather, S. M., 1994, $^{40}Ar/^{39}Ar$ geochronology of basaltic rocks and constraints on Late Cenozoic stratigraphy and landscape development in the Red Hill-Quemado area, New Mexico: New Mexico Geological Society, 45th Field Conference, Guidebook, p. 209-215.

McKenzie, D., 1989, Some remarks on the movement of small melt fractions in the mantle: Earth and Planetary Science letters, v. 95, p. 53-72.

McMillan, N. J., 1998, Temporal and spatial magmatic evolution of the Rio

Grande rift: New Mexico Geological Society, 49th Field Conference, Guidebook, p. 116.

Menzies, M. A., Kyle, P. R., Jones M. and Ingram, G., 1991, Enriched and depleted source components for tholeiitic and alkaline lavas from Zuni-Bandera, New Mexico: Inferences about intraplate processes and stratified lithosphere: Journal of Geophysical Research, v. 96-B8, p. 13,645-13,671.

Minier, J. and Reiter, M., 1991, Heat flow on the southern Colorado Plateau: Tectonophysics, v. 200, p. 51-66.

Moore, J. G. and Evans, B. W., 1967, The role of olivine in the crystallization of the prehistoric Makaophui tholeiitic lava lake, Hawaii: Contributions to Mineralogy and Petrology, v. 15, p. 202-223.

Nakamura, N., 1974, Determination of REE, Ba, Fe, Mg, Na and K in carbonaceous and ordinary chondrites: Geochimica et Cosmochimica Acta, v. 38, p. 757-775.

Norrish, K. and Chappell, B. W., 1977, X-ray fluorescence spectrometry, *in* Zussman, J., ed., Physical Methods in Determinative Mineralogy: London, Academic Press, p. 201-273.

Osborne, F. F. and Roberts, E. J., 1931, Differentiation in the Shonkin Sag laccolith, Montana: American Journal of Science, v. 22, p. 331-353.

Perry, F. V., Baldridge, W. S. and DePaolo, D. J., 1987, Role of Asthenosphere and lithosphere in the genesis of Late Cenozoic basaltic rocks from the Rio Grande Rift and adjacent regions of the Southwestern United States: Journal of Geophysical Research, v. 92-B9, p. 9193-9213.

Peterson, D. W. and Moore, R. B., 1987, Geologic history and evolution of geologic concepts, Island of Hawaii, *in* Decker, R. W., Wright, T. L. and Stauffer, P. H., eds., Volcanism in Hawaii.: Washington, U. S. Geological Survey Professional Paper 1350, p. 149-189.

Philpotts, A. R., 1990, Principles of Igneous and Metamorphic Petrology: Englewood Cliffs, Prentice Hall, 498 p.

Philpotts, A. R. and Carroll, M., 1996, Physical properties of partly melted tholeiitic basalt: Geology, v. 24, p. 1029-1032.

Philpotts, A. R., Carroll, M. and Hill, J. M., 1996, Crystal-mush compaction and the origin of pegmatitic segregation sheets in a thick flood-basalt flow in the Mesozoic Hartford Basin, Connecticut: Journal of Petrology, v. 37, p. 811-836.

Pouchou, J. L. and Pichoir, F., 1985, "PAP" $\phi(\rho z)$ procedure for improved quantitative microanalysis, *in* Armstrong, J. T., ed., Microbeam Analysis—1985: San Francisco, San Francisco Press, p. 104.

Puffer, J. H. and Horter, D. L., 1993, Origin of pegmatitic segregation veins within flood basalts: Geological Society of America Bulletin, v. 105, p. 738-748.

Reid, M. R., Hart, S. R., Padovani, E. R., and Wandless, G. A., 1989, Contribution of metapelitic sediments to the composition, heat production, and seismic velocity of the lower crust of southern New Mexico, U.S.A: Earth and Planetary Science Letters, v. 95, p. 367-381.

Saemundsson, K., 1979, Outline of the geology of Iceland: Jokull, v. 29, p. 7-28.

Stormer, J. C., Jr., 1973, Calcium zoning in olivine and its relationship to silica activity and pressure: Geochimica et Cosmochimica Acta, v. 37, p. 1815-1821.

Stormer, J. C., Jr., 1983, The effects of recalculation on estimates of temperature and oxygen fugacity from analyses of multicomponent iron-titanium oxides: American Mineralogist, v. 68, p. 586-594.

Stormer, J. C., Jr., and Nicholls, J., 1978, XLFRAC: A program for interactive testing of magmatic differentiation models: Computers and Geosciences, v. 4, p. 143-159.

Sun, S. S. and McDonough, W. F., 1989, Chemical and isotopic systematics of oceanic basalts: implications for mantle composition and processes, *in* Saunders, A. D. and Norry, M. J., eds., Magmatism in the Ocean Basins: Geological Society Special Publication 42, pp. 313-345.

Thompson, R. N., Morrison, M. A., Hendry, G. L. and Parry, S. J., 1984, An assessment of the relative roles of crust and mantle in magma genesis: an elemental approach: Philosophical Transactions of the Royal Society of London, v. A310, p. 549-590.

Tatsumi, Y., 1989, Migration of fluid phases and genesis of basalt magmas in subduction zones: Journal of Geophysical Research, v. 94-B4, p. 4697-4707.

van der Molen, I. and Paterson, M. S., 1979, Experimental deformation of partially-melted granite: Contributions to Mineralogy and Petrology, v. 70, p. 299-318.

Wilson, M., 1989, Igneous Petrogenesis: London, Harper Collins Academic, 466 p.

Wright, T. L. and Okamura, R. T., 1977, Cooling and cry stallization of tholeiitic basalt, 1965 Makaopuhi lava lake, Hawaii: U. S. Geological Survey Professional Paper 1004, 78 p.

Zindler, A. and Hart, S, 1986, Chemical geodynamics: Annual Reviews in Earth and Planetary Science, v. 14, p. 493-571.